

## ORIGINAL ARTICLE

# Murine LRBA deficiency causes CTLA-4 deficiency in Tregs without progression to immune dysregulation

Deborah Burnett<sup>1</sup>, Ian Parish<sup>2</sup>, Etienne Masle-Farquhar<sup>1</sup>, Robert Brink<sup>1</sup> and Christopher Goodnow<sup>1</sup>

Inherited mutations in lipopolysaccharide-responsive beige-like anchor (*LRBA*) cause a recessive human immune dysregulation syndrome with memory B-cell and antibody deficiency (common variable immunodeficiency), inflammatory bowel disease, enlarged spleen and lymph nodes, accumulation of activated T cells and multiple autoimmune diseases. To understand the pathogenesis of the syndrome, C57BL/6 mice carrying a homozygous truncating mutation in *Lrba* were produced using CRISPR/Cas9-mediated gene targeting. These mice revealed that LRBA has a critical, cell-autonomous role in promoting cytotoxic T-lymphocyte antigen-4 (CTLA-4) accumulation within CD4 effector T cells and FOXP3<sup>+</sup> T-regulatory cells (Tregs). In young mice, or in chimeric mice where only half of the T cells are LRBA deficient, low CTLA-4 was the only detectable abnormality in Tregs, whereas in old mice FOXP3 was also decreased. Low CTLA-4 did not translate into increased CD86 on B cells unless the LRBA-deficient mice were immunised, and neither immunisation nor chronic lymphocytic choriomeningitis virus infection precipitated immune dysregulation. LRBA deficiency did not alter antigen-specific B-cell activation, germinal centre (GC) formation, isotype switching or affinity maturation. Paradoxically, CD86 was decreased on GC B cells in LRBA-deficient mice, pointing to compensatory mechanisms for controlling CD86 in the face of low CTLA-4. These results add to the experimental rationale for treating LRBA deficiency with the CTLA4-Ig fusion protein, Abatacept, and pose questions about the limitations of laboratory experiments in mice to reproduce human disease *in natura*.

*Immunology and Cell Biology* (2017) 00, 1–14. doi:10.1038/icb.2017.50

Lipopolysaccharide-responsive beige-like anchor (LRBA) belongs to the BEACH (*beige* and *Chediak-Higashi* syndrome) family of cytoplasmic proteins that regulate intracellular vesicle trafficking and exocytosis.<sup>1</sup> LRBA was originally identified as the product of a human gene with homology to yeast CDC4,<sup>2</sup> and of an LPS-induced gene in mouse pre-B cells.<sup>3</sup> Homozygous loss-of-function *LRBA* mutations were discovered in 2012 as the cause of a new human immunodeficiency disorder characterised by recurrent infections and defects in B-lymphocyte activation, low numbers of isotype-switched memory B cells and diminished IgG and IgA antibody formation<sup>4</sup> and by chronic diarrhoea.<sup>5</sup> Subsequently, homozygous or compound heterozygous *LRBA*-inactivating mutations have been found to cause a pleiotropic immune dysregulation syndrome with recessive Mendelian inheritance.<sup>4–17</sup> In two studies comparing 31<sup>6</sup> and 22<sup>18</sup> LRBA-deficient patients, the most common clinical features were autoimmune disease, particularly haemolytic anaemia (12/31 and 12/21 patients) and immune thrombocytopenic purpura (9/31 and 11/21 patients), splenomegaly or lymphadenopathy (19/31 and 18/21 patients), enteropathy or chronic diarrhoea (19/31 and 13/21 patients) that was mostly idiopathic, and recurrent upper and lower respiratory tract infections (19/31 and 10/19).<sup>6,18</sup> Immune dysregulation caused by LRBA deficiency has a broad range of other autoimmune manifestations, but in one form or another appears to have high

clinical penetrance in the first decade of life with only two recorded clinical cases of homozygous *LRBA* mutations without clinical disease, although this may relate to difficulty in detecting asymptomatic individuals.<sup>6,12</sup> The pathogenesis of immunodeficiency and autoimmunity caused by LRBA deficiency is not understood.

Laboratory findings from children with LRBA deficiency are also variable in presentation and raise many questions about pathogenesis.<sup>6,18</sup> Hypogammaglobulinemia is found in 57–58% of patients.<sup>6,18</sup> Total B-lymphocyte counts are often normal or sometimes reduced, but isotype-switched memory B cells are decreased in >80% of patients<sup>6,18</sup> and plasmablasts are reduced in 92% of patients.<sup>18</sup> Natural killer (NK) cells are normal or decreased in LRBA patients.<sup>6,18</sup> Counts of CD4<sup>+</sup> and CD8<sup>+</sup> T cells are generally normal; however, individual patients have presented with either increases or decreases in their numbers,<sup>6,18</sup> and the percentage of CD45RO<sup>+</sup> RA<sup>-</sup> activated/memory T cells and CXCR5<sup>+</sup> PD-1<sup>+</sup> follicular helper T cells is increased.<sup>8</sup> FOXP3<sup>+</sup> CD4<sup>+</sup> T-regulatory (Treg) cells are decreased as the percentage of CD4<sup>+</sup> cells in the majority of LRBA-deficient patients<sup>6,8,18</sup> and the Tregs that are present have decreased levels per cell of FOXP3, HELIOS, CD25 and CTLA-4 (cytotoxic T-lymphocyte antigen-4).<sup>8,11</sup> These pleiotropic lymphocyte abnormalities, together with the broad expression of *LRBA* mRNA across leucocyte subsets and other tissues, make it unclear if LRBA deficiency

<sup>1</sup>Immunology Division, Garvan Institute for Medical Research, Sydney, NSW, Australia and <sup>2</sup>John Curtin School of Medical Research, Australian National University, Canberra, ACT, Australia

Correspondence: Professor C Goodnow, Immunology Division, Garvan Institute for Medical Research, 384 Victoria Street, Sydney, NSW 2010, Australia.

E-mail: c.goodnow@garvan.org.au

Received 13 March 2017; revised 6 June 2017; accepted 6 June 2017

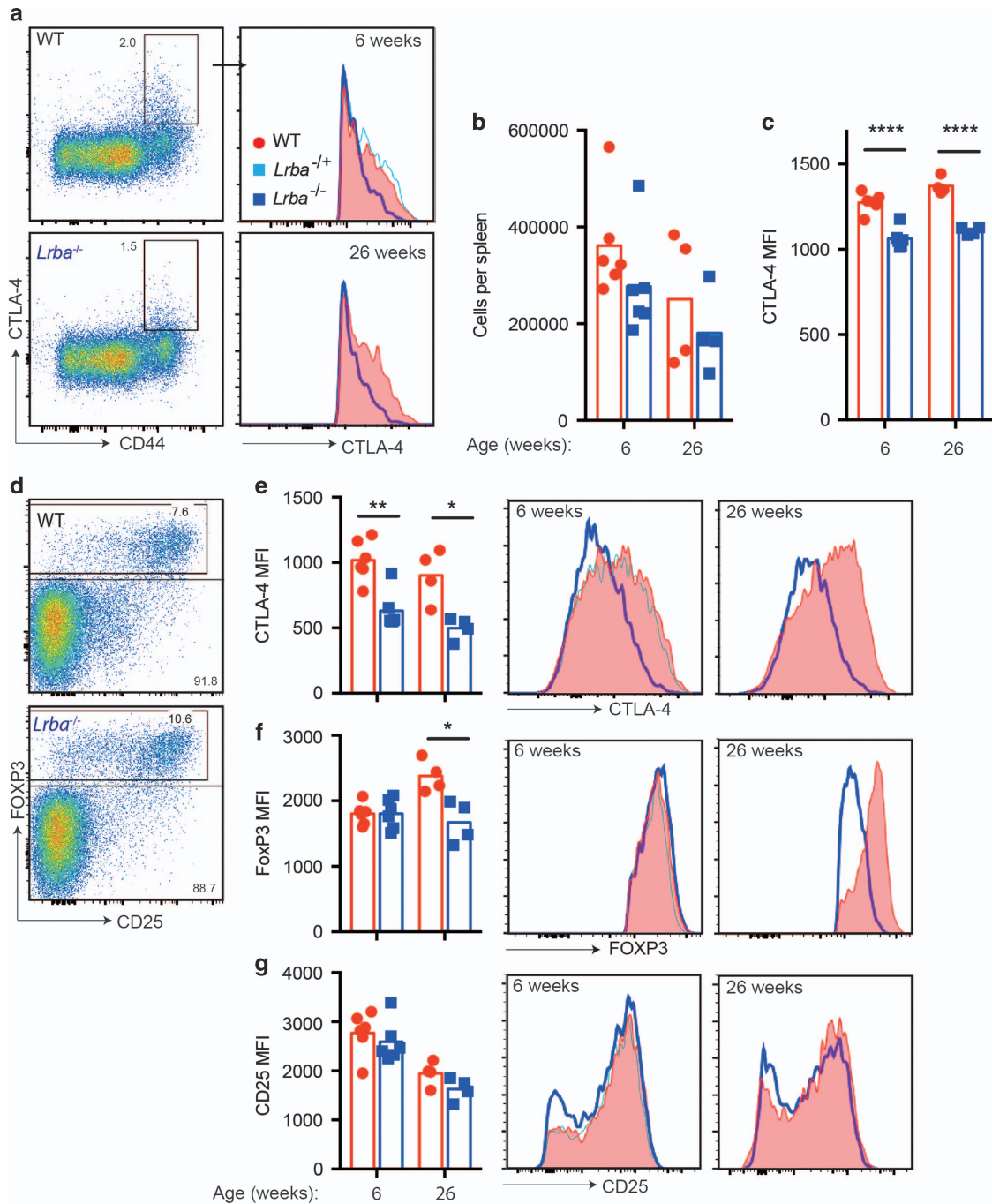


**Figure 1** LRBA deficiency decreases CTLA-4 on CD4 effector/memory and Tregs. Flow cytometric analysis of spleen cells from age- and sex-matched *Lrba*<sup>-/-</sup> (blue) or WT (red) mice at 6 (*n*=6) or 26 weeks (*n*=4) of age. **(a–c)** CTLA-4 expression on CD4 memory/effector T cells. **(a)** Representative flow cytometry plots of permeabilised CD4<sup>+</sup> FOXP3<sup>-</sup> cells from 6-week-old mice showing % CTLA-4<sup>+</sup> CD44<sup>hi</sup> cells and histograms of CTLA-4 in the CD4<sup>+</sup> CD44<sup>hi</sup> CTLA-4<sup>+</sup> population in 6- and 26-week-old mice. *Lrba*<sup>-/+</sup> are indicated in pale blue. Graphs show **(b)** the number of CTLA-4<sup>+</sup> CD4<sup>+</sup> CD44<sup>hi</sup> FOXP3<sup>-</sup> cells and **(c)** CTLA-4 mean fluorescence intensity (MFI) in individual mice and arithmetic mean for each genotype and age group. **(d–g)** CTLA-4 expression on CD4<sup>+</sup> Treg cells. **(d)** Representative plots of permeabilised CD4<sup>+</sup> cells showing the % FOXP3<sup>+</sup> Treg cells in 6-week-old mice. Representative Treg histograms and MFI for: **(e)** CTLA-4; **(f)** FOXP3; **(g)** CD25. Statistical analysis was carried out using *t*-test: \**P*<0.05; \*\**P*<0.01; \*\*\**P*<0.001; \*\*\*\**P*<0.0001. Data are representative of one experiment.

causes intrinsic deficits in B-cell isotype switching and memory formation,<sup>4</sup> a primary, generalised deficit in FOXP3<sup>+</sup> Treg cells,<sup>8</sup> or a problem in nonlymphoid organs such as the gut.

An important insight into the pathogenesis of LRBA-deficiency syndrome came from the finding in 2015 that the immune dysregulation responds exceptionally well to treatment with soluble CTLA4-Ig

fusion protein, Abatacept.<sup>11</sup> Experimental analysis of cells in culture revealed that CTLA-4 and LRBA interact through specific sequences in the CTLA-4 cytoplasmic tail, localise at recycling endosomes and the trans-Golgi network, and that LRBA protects CTLA-4 from being sorted to and degraded in lysosomes.<sup>11</sup> Hence, an attractive hypothesis is that low CTLA-4 expression on activated T cells or FOXP3<sup>+</sup> Treg

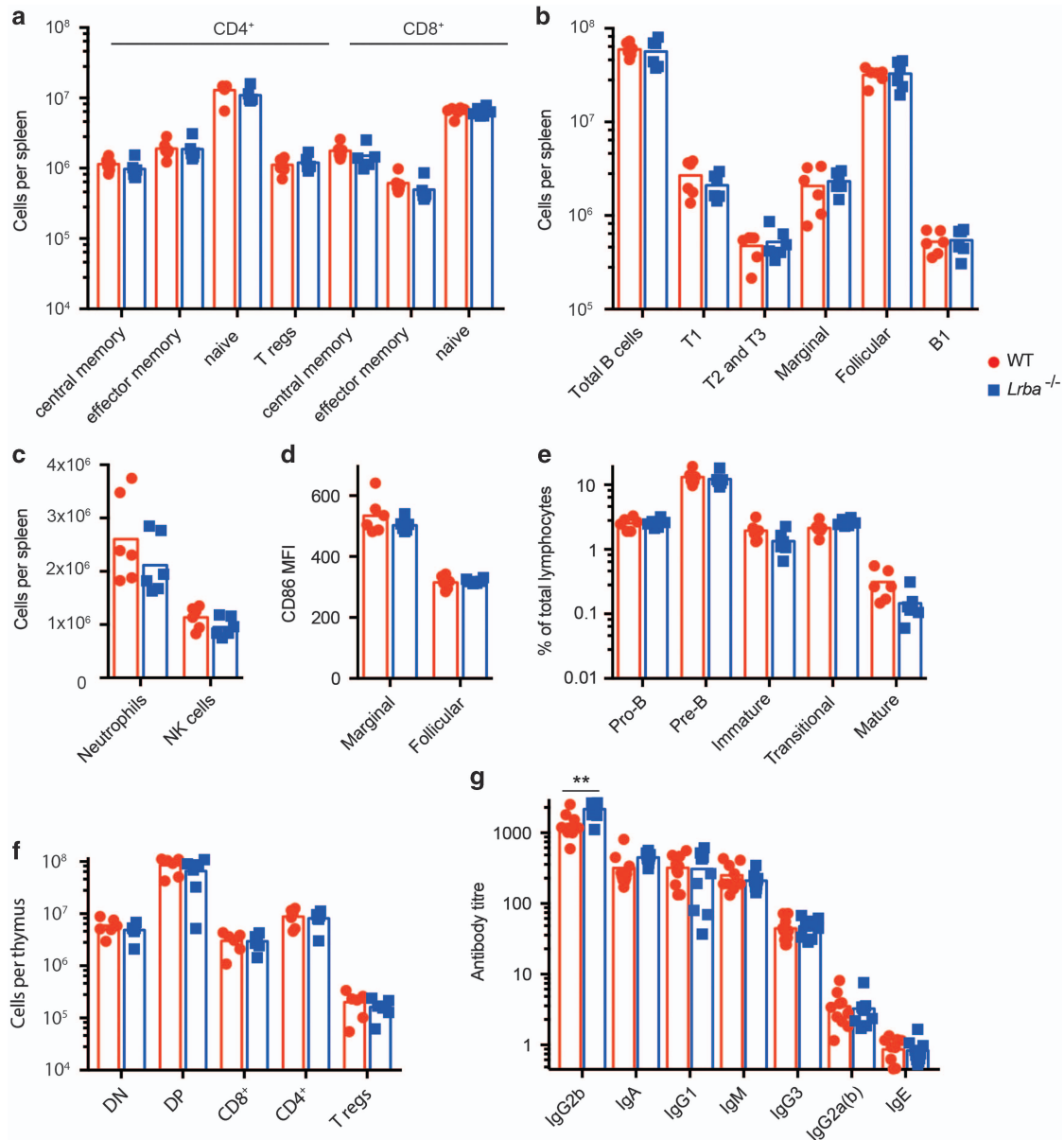


**Figure 2** Absence of immune dysregulation disease in LRBA-deficient mice. (a–f) Analysis of sex-matched WT (red) and *Lrba*<sup>-/-</sup> (blue) mice at 6 weeks of age, showing individual results and means for each group. (a–c) Flow cytometric analysis of spleen, showing the numbers of: (a) CD4<sup>+</sup> or CD8<sup>+</sup> T-cell subsets of central memory (CD62L<sup>+</sup> CD44<sup>+</sup>), effector memory (CD62L<sup>-</sup> CD44<sup>+</sup>), naïve (CD62L<sup>+</sup> CD44<sup>-</sup>) or Tregs (CD4<sup>+</sup> FOXP3<sup>+</sup>). (b) B cells (B220<sup>+</sup>) and subsets of transitional 1 (T1, B220<sup>+</sup> CD93<sup>+</sup> CD23<sup>-</sup>), transitional 2 and 3 (B220<sup>+</sup> CD93<sup>+</sup> CD23<sup>+</sup>), marginal zone (B220<sup>+</sup> CD21<sup>+</sup> CD23<sup>-</sup>), mature follicular (B220<sup>+</sup> CD93<sup>-</sup> CD23<sup>+</sup>) and B-1 (B220<sup>-</sup> CD19<sup>+</sup>) B cells per spleen. (c) neutrophils (B220<sup>-</sup> MHC II<sup>-</sup> Ly6G<sup>+</sup> CD11b<sup>+</sup>) and NK lymphocytes (B220<sup>-</sup> CD8<sup>-</sup> MHC II<sup>-</sup> NK1.1<sup>+</sup>). (d) CD86 mean fluorescence intensity (MFI) on marginal zone and follicular B cells. (e) Flow cytometric analysis of bone marrow, showing % of lymphocytes that are pro-B cells (B220<sup>+</sup> CD43<sup>int</sup>), pre-B cells (B220<sup>+</sup> CD43<sup>-</sup> IgM<sup>-</sup>), immature B cells (B220<sup>int</sup> CD43<sup>-</sup> IgM<sup>+</sup> IgD<sup>-</sup>), transitional B cells (B220<sup>hi</sup> CD43<sup>-</sup> IgM<sup>+</sup> CD24<sup>-</sup> IgD<sup>lo</sup>) and mature B cells (B220<sup>hi</sup> CD43<sup>-</sup> IgM<sup>+</sup> CD24<sup>-</sup> IgD<sup>+</sup>). (f) Flow cytometric analysis of thymus, showing number of CD8<sup>-</sup> CD4<sup>-</sup> double-negative (DN), double-positive (DP), CD8<sup>+</sup> or CD4<sup>+</sup> single-positive, or CD4<sup>+</sup> FoxP3<sup>+</sup> Treg cells. *N* = 6 per group. Data are representative of one experiment. (g) Titres of IgG2b, IgA, IgG1, IgM, IgG3 Ig2Ga(b) and IgE antibodies in the serum of unimmunised mice, determined by enzyme-linked immunosorbent assay (ELISA). *N* = 10 per group. Representative of two comparable experiments. Statistical analysis was carried out using *t*-test: \*\**P* < 0.01.

cells is responsible for some or all of the immune dysregulation in LRBA deficiency. CTLA-4 on T cells removes CD86 from antigen-presenting cells,<sup>19</sup> and exaggerated expression of CD86 on anergic self-reactive B cells switches the outcome of their interaction with T cells from FAS-mediated deletion to plasma cell differentiation and autoantibody secretion,<sup>20</sup> providing a plausible mechanism for the pathogenesis of autoimmune haemolytic anaemia and thrombocytopenia and its correction with Abatacept therapy. However, it is unclear

how this mechanism would explain the humoral immunodeficiency and low numbers of switched memory B cells, which appear less responsive to Abatacept.<sup>11</sup>

To resolve the many questions summarised above, we generated and analysed an LRBA-deficient mouse strain. The results reveal no evidence for an intrinsic requirement for LRBA in B-cell activation, germinal centre (GC) formation, isotype switching and affinity maturation. LRBA deficiency greatly decreased CTLA-4 on activated

CD4<sup>+</sup> T cells and FOXP3<sup>+</sup> Tregs in a cell-autonomous manner, but other Treg markers and Treg frequency were unaffected in young mice. We conclude that partial CTLA-4 deficiency is a primary component of the immune dysregulation that occurs in LRBA deficiency, but is compensated to prevent progression to autoimmunity and immunodeficiency under standard mouse housing conditions.

## RESULTS

### CTLA-4 deficiency in T cells of LRBA-deficient mice

LRBA-deficient mice were generated on the C57BL/6 background using CRISPR/Cas9-mediated gene targeting to produce an 8 bp deletion in exon 37 of *Lrba*. The resulting frame-shift mutation truncates the normal protein sequence starting at His1949 within the DUF domain, eliminating the C-terminal PH, BEACH and WD40 domains as occurs in many patients with LRBA deficiency, including individuals with good response to Abatacept.<sup>6,11,18</sup> Multiple homozygous founders were obtained, and these appeared healthy, fertile and were outcrossed to C57BL/6 mice and progeny intercrossed to establish a propagating strain.

Flow cytometric analysis of permeabilised T cells in the blood (not shown) or spleen (Figure 1) of homozygous LRBA-deficient mice revealed a loss of CTLA-4<sup>hi</sup> cells in CD4<sup>+</sup> CD44<sup>+</sup> T cells (Figures 1a–c) and in FOXP3<sup>+</sup> Tregs (Figures 1d and e), regardless of the age of the mice analysed. In Tregs, the CTLA-4 mean fluorescence intensity was decreased in homozygous mutants to ~60% of wild-type (WT) levels in the spleen (Figure 1e) and thymus (Supplementary Figure 1). FOXP3 and CD25 were expressed normally in Tregs from young LRBA-deficient mice, but FOXP3 was decreased in both the spleen (Figure 1f) and thymus of 6-month-old mice (Supplementary Figure 1). Thus, Tregs exhibited a selective CTLA-4 deficiency in young LRBA-deficient mice, whereas older mice displayed a broader decrease in CTLA-4, FOXP3 as observed in human LRBA deficiency.<sup>8,11</sup>

### No spontaneous immune dysregulation disease in LRBA-deficient mice

In contrast to the morbid immune dysregulation in human LRBA deficiency, LRBA-deficient mice developed at normal frequencies with no obvious morphological abnormalities, normal body weight, normal erythrocyte and platelet counts, and no splenomegaly, whether analysed at 6 weeks of age or at 6 months of age (Figure 2 and Supplementary Figure 2). There was also no lymphadenopathy (not shown). Flow cytometric analysis of the spleen revealed normal numbers of neutrophils, NK cells, B-cell subsets or T-lymphocyte subsets, with no increase in effector/memory T cells or decrease in Tregs as has been observed in LRBA-deficient patients. Based on the low levels of CTLA-4 on Treg and effector T cells, we tested for increased CD86 on the surface of B cells, but found it to be comparable in young mice with or without LRBA (Figure 2d). We also investigated the expression of BTLA, a homologue of CTLA-4, on total B cells and GC B cells. However unlike CTLA-4, BTLA expression was not decreased on lymphocytes from LRBA-deficient mice (Supplementary Figure 2E). Developing subsets of B and T cells in the bone marrow and thymus were present in normal numbers (Figures 2e and f), despite the low expression of CTLA-4 on thymic Tregs.

To investigate potential disease progression over time, mice were also analysed at 6 months of age (Supplementary Figure 2). Older LRBA-deficient mice appeared normal in regards to their total body weight and frequencies of red blood cells, platelets, neutrophils, NK

cells and B- and T-cell subsets and development. Interestingly, we did notice a slight but significant decrease in B220<sup>lo</sup> CD19<sup>+</sup> B-1 cells within the spleen that was not evident in the younger mice (Supplementary Figures 2L and M).

### LRBA mice show altered frequencies in the serum of antibody isotypes

Given hypogammaglobulinemia is a frequent clinical feature of human *Lrba* deficiency, we measured basal Ig levels in the serum of *Lrba*<sup>-/-</sup> and WT mice. This revealed the serum of unimmunised *Lrba*<sup>-/-</sup> mice to contain significantly higher levels of IgG2b than age- and sex-matched WT mice (Figure 2g). There was also a trend towards an increase in IgM levels, although this was not significant ( $P=0.056$ ).

### Peritoneal B-1 cells are reduced in *Lrba*<sup>-/-</sup> mice

Given the finding that LRBA-deficient mice aged >6 months of age have a reduced frequency of splenic B-1 cells and in light of the chronic diarrhoea and IBD occurring in 60% of LRBA-deficient patients, we tested for cellular abnormalities in the peritoneal fluid of LRBA-deficient mice. This revealed a significant relative decrease in B-1 cells (CD19<sup>+</sup> B220<sup>lo</sup> IgM<sup>+</sup> CD23<sup>-</sup>) with no corresponding decrease in B-2 cells (CD19<sup>-</sup> B220<sup>hi</sup>) in both 6-week-old and 6-month-old LRBA-deficient mice (Figure 3). This decrease was largely due to decreased B-1a cells (CD19<sup>+</sup> B220<sup>lo</sup> IgM<sup>+</sup> CD23<sup>-</sup> CD5<sup>+</sup>). Interestingly, T cells were increased relative to other cell types within the peritoneal compartment in young and aged LRBA-deficient mice, although this could have been secondary to decreased B-1 cells.

### Primary effects of LRBA deficiency within different subsets of lymphocytes after bone marrow transplantation

To investigate the possibility that homeostatic compensation mechanisms mask cell-autonomous deficits in LRBA-deficient T or B cells, mixtures of *Lrba*<sup>-/-</sup> and WT bone marrow distinguished by CD45.2 and CD45.1 congenic markers were transplanted to lymphocyte-deficient *Rag1*<sup>-/-</sup> mice. The marrow transplant competitively reconstituted the immune system with a mixture of cells with and without LRBA expression. A control group of recipients were transplanted with marrow mixtures where both CD45.2 and CD45.1 cells had normal LRBA expression. A third group of recipients were reconstituted with 100% CD45.2 marrow that was either *Lrba*<sup>-/-</sup> or *Lrba*<sup>+/+</sup>. The resulting chimeric animals were immunised repeatedly with sheep red blood cells (SRBCs), and blood lymphocytes were analysed by flow cytometry. Despite competing with CD45.1 WT cells, *Lrba*<sup>-/-</sup> CD45.2<sup>+</sup> cells accounted for a high percentage of B cells, CD4<sup>+</sup> T cells, CD8<sup>+</sup> T cells, effector CD4<sup>+</sup> T cells, effector CD8<sup>+</sup> T cells and Treg cells (Figure 4a). The contribution of LRBA-deficient CD45.2<sup>+</sup> cells to each subset was equivalent to the contribution of WT CD45.2<sup>+</sup> cells in control mixed chimera animals analysed at the same time (Figure 4a), and this was true for blood samples collected at multiple timepoints before and after repeated SRBC immunisation (Supplementary Figures 3 and 4).

Despite normal contribution of LRBA-deficient CD45.2<sup>+</sup> cells to the CD4<sup>+</sup> memory/effector and Treg cell populations, they exhibited a selective and marked decrease in the total (intracellular and surface) cellular pool of CTLA-4. Within FOXP3<sup>-</sup> CD4<sup>+</sup> cells, CTLA-4 was highly expressed in a subset of CD44<sup>hi</sup> effector/memory cells in *Lrba*<sup>+/+</sup> T-cell populations, but CTLA-4<sup>+</sup> cells were 80% less frequent among CD45.2<sup>+</sup> *Lrba*<sup>-/-</sup> T cells (Figures 4b and c). Furthermore, in the CTLA-4<sup>+</sup> CD44<sup>hi</sup> cells that were present, these expressed CTLA-4 at mean intensities that were only 40% of CD45.1<sup>+</sup> internal control cells and of WT CD45.2<sup>+</sup> cells in control mixed chimeras (Figures 4d and e). Among FOXP3<sup>+</sup> CD4<sup>+</sup> Treg cells, CD45.2<sup>+</sup> *Lrba*<sup>-/-</sup> Tregs

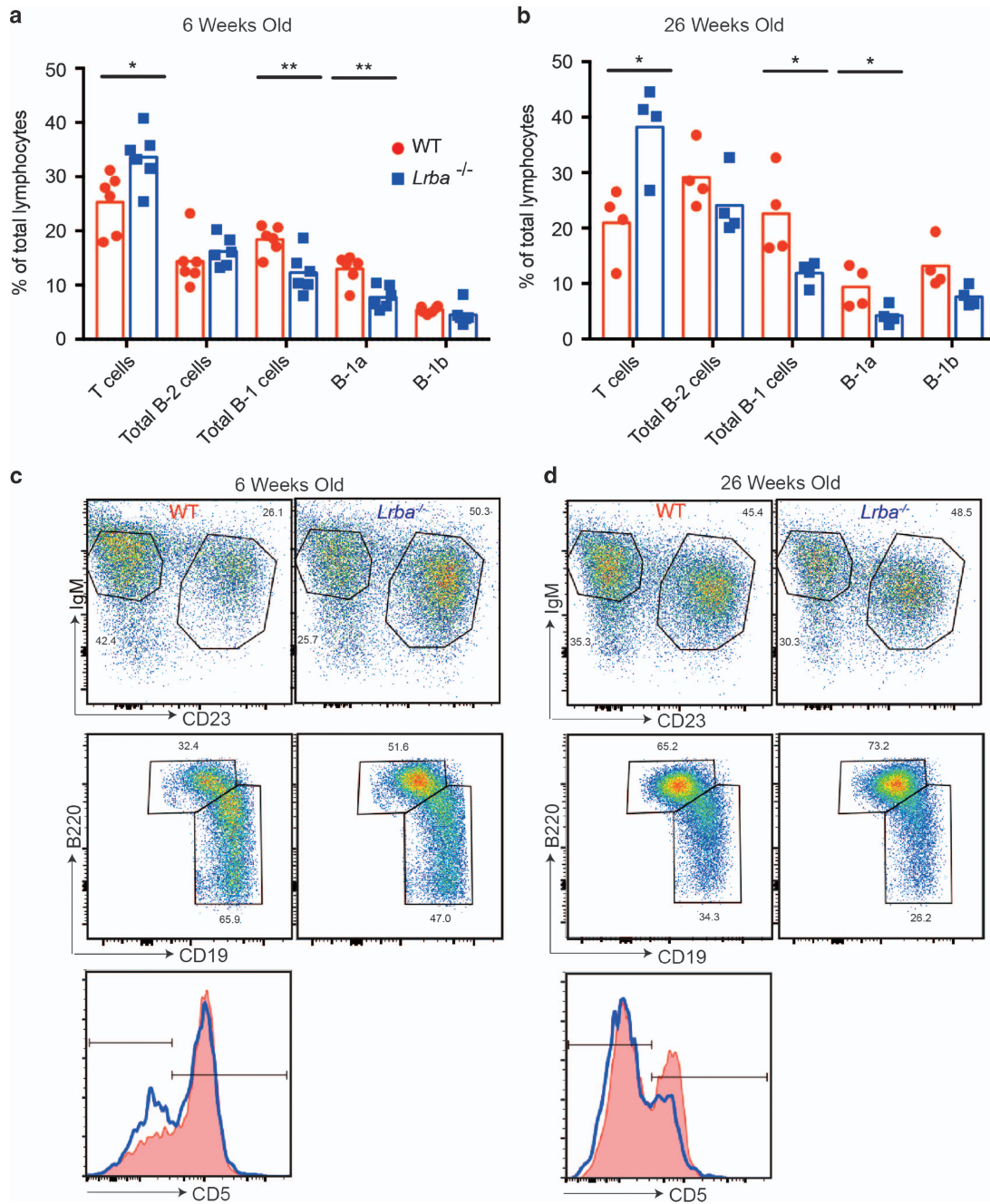


**Figure 3** Decreased peritoneal B-1 B cells in LRBA-deficient mice. Flow cytometric analysis of peritoneal cavity lymphocytes from sex-matched WT (red) and *Lrba*<sup>-/-</sup> (blue) mice at 6 ( $n=6$ ) or 26 ( $n=4$ ) weeks of age, showing individual results and means for each group. (a and b) Percentage of lymphocytes that are T cells (B220<sup>-</sup> IgM<sup>-</sup> CD23<sup>-</sup> CD5<sup>+</sup>), B-2 cells (CD19<sup>-</sup> B220<sup>hi</sup>), B-1 cells (CD19<sup>+</sup> B220<sup>lo</sup> IgM<sup>+</sup> CD23<sup>-</sup>), B-1a cells (CD19<sup>+</sup> B220<sup>lo</sup> IgM<sup>+</sup> CD23<sup>-</sup> CD5<sup>+</sup>) and B-1b cells (CD19<sup>+</sup> B220<sup>lo</sup> IgM<sup>+</sup> CD23<sup>-</sup> CD5<sup>-</sup>). (c and d) Representative flow cytometric plots showing gating IgM, CD23, B220 and CD19 staining for B-1 and B-2 cells and representative CD5 histograms of B-1 cells showing gates on CD5<sup>+</sup> B-1a and CD5<sup>-</sup> B-1b cells from mice at 6 (c) and 26 (d) weeks of age. Statistical analysis was carried out using *t*-test: \* $P < 0.05$ ; \*\* $P < 0.01$ . Data are representative of one experiment.

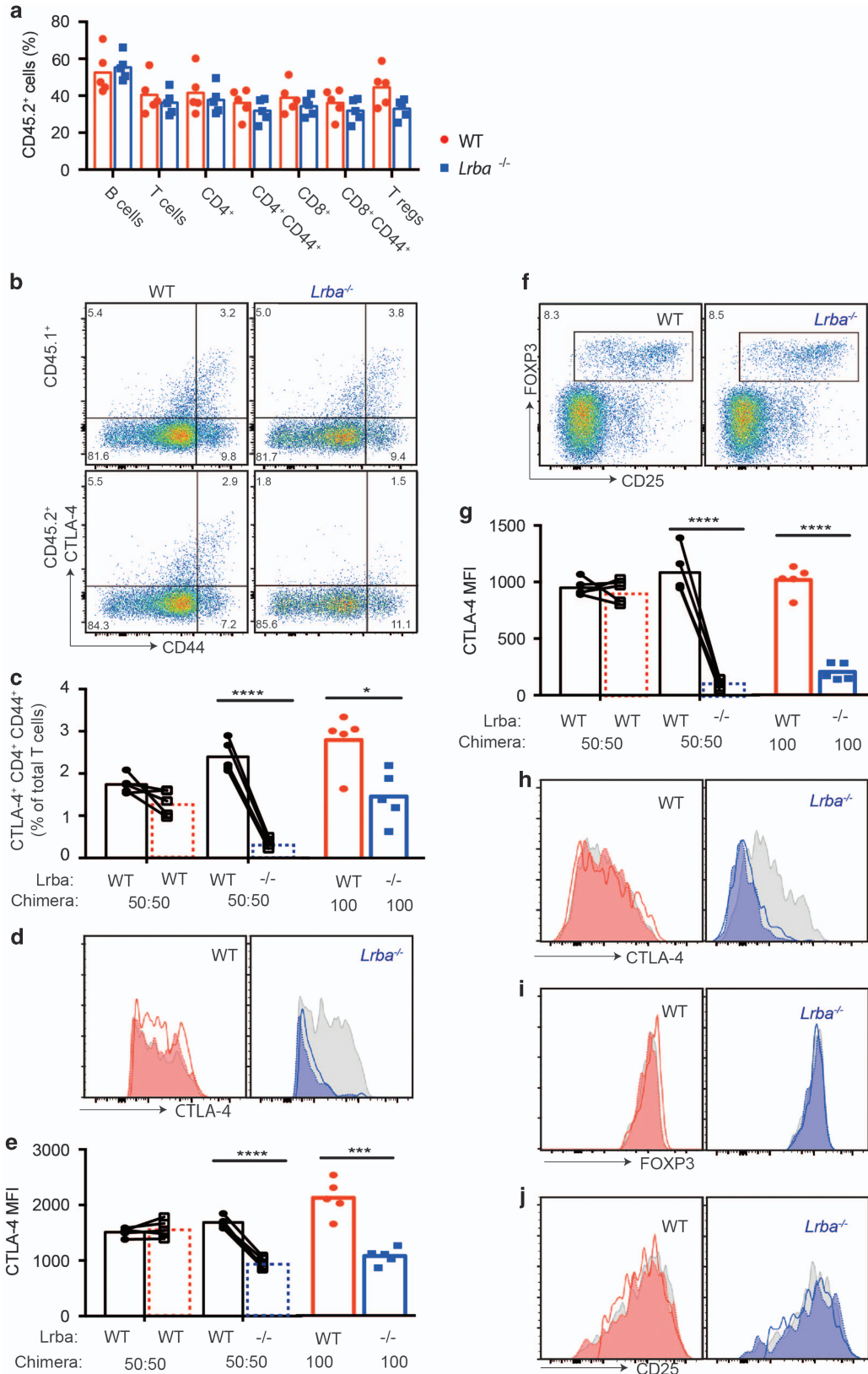
expressed CTLA-4 at mean intensities that were only 10% of CD45.1<sup>+</sup> internal control cells or of WT CD45.2<sup>+</sup> cells in control mixed chimeras (Figures 4g and h). By contrast, there was no decrease in FOXP3 or CD25 in CD45.2<sup>+</sup> *Lrba*<sup>-/-</sup> Tregs (Figures 4i and j). These results demonstrate that the loss of CTLA-4 protein caused by LRBA deficiency is cell autonomous within Treg and helper T cells. The loss of CTLA-4 was similar in chimeras where only half the Tregs were LRBA deficient and in chimeric mice where all cells were defective (Figures 4e and h).

#### Potent immune activation by xenoantigens or virus infection fails to precipitate immune dysregulation in LRBA-deficient mice

The experiments above showed loss of normal CTLA-4 protein caused by LRBA deficiency, but it was surprisingly not accompanied by the morbid immune dysregulation observed in CTLA-4-knockout mice.<sup>21,22</sup> We hypothesised that the residual CTLA-4 in LRBA-deficient Tregs might become insufficient in the face of potent inducers of CD80 and CD86 on dendritic cells and B cells. We first tested this possibility by repeatedly injecting SRBCs, which induces

potent dendritic cell activation, CD86 induction, follicular helper T-cell and GC B-cell proliferation because they carry numerous xenoantigens and sheep CD47 does not bind mouse SIRP $\alpha$  and fails to deliver the inhibitory signal carried by healthy self-erythrocytes.<sup>23</sup> In

the experiments above, a parallel set of *Rag1*<sup>-/-</sup> recipients were transplanted with 100% *Lrba*<sup>-/-</sup> or *Lrba*<sup>+/+</sup> CD45.2 bone marrow, so that all T cells were LRBA deficient or sufficient. CTLA-4 was decreased on the *Lrba*<sup>-/-</sup> Tregs to 30% of the levels on *Lrba*<sup>+/+</sup> Tregs.



Despite the loss of normal CTLA-4 on 100% of the Tregs, there was no evidence of immune dysregulation syndrome and no increased formation of CD44<sup>hi</sup> CD4 or CD8 effector/memory T cells either before or following three sequential immunisations with SRBCs (Supplementary Figure 4B).

To test if a systemic viral infection would precipitate immune dysregulation, *Lrba*<sup>-/-</sup> mice and age- and sex-matched WT control mice were infected with lymphocytic choriomeningitis virus (LCMV) clone 13, which multiplies to high viral titres throughout the body peaking within 7 days, establishes a chronic viral infection and induces powerful innate and adaptive immune activation during the acute and chronic phase of the infection. Following infection, *Lrba*<sup>-/-</sup> mice exhibited no visible evidence of morbidity and were indistinguishable from their WT counterparts. Measured by flow cytometry, the immune response to LCMV infection 20 days after infection was remarkably normal, with no significant difference in the percentage of CD4<sup>+</sup> T cells that were effector/memory cells (Figure 5a) nor in the percentage of CD4<sup>+</sup> or CD8<sup>+</sup> T cells that bound major histocompatibility complex (MHC) tetramers containing the dominant viral peptides (Figures 5b and c). Rather than developing autoimmunity or exaggerated formation of effector T cells, we found that *Lrba*<sup>-/-</sup> mice actually showed subtle signs of increased T-cell exhaustion compared with their WT counterparts. This included a slight but significant decrease in effector CD8<sup>+</sup> T cells, and changes in markers of T-cell exhaustion<sup>24</sup> on viral peptide/MHC tetramer-binding T cells including increased TIM3 and decreased Ly6C (Figures 5b and c), slightly decreased mean interferon- $\gamma$  per cell and decreased the proportion of tumour necrosis factor- $\alpha$ -positive cells (Figures 5d and e). Nevertheless, the key finding from these experiments is that LRBA-deficient mice mount a remarkably normal immune response to a chronic, systemic viral infection.

#### LRBA-deficient B cells undergo normal affinity maturation

Given the decreased frequency of switched memory B cells in the majority of LRBA-deficient patients, we investigated whether or not LRBA-deficient B cells would respond normally to antigenic stimulation *in vivo*. To do this, *Lrba*<sup>-/-</sup> C57BL/6 mice were crossed to SW<sub>HEL</sub> IgH knock-in transgenic mice where many B cells express the Hy10 antibody against hen egg lysozyme (HEL).<sup>25,26</sup> CD45.1 congenic mice with normal LRBA were injected intravenously with 30 000 HEL-binding spleen cells from CD45.2 SW<sub>HEL</sub> donor mice, where the donors were either *Lrba*<sup>-/-</sup> or *Lrba*<sup>+/+</sup>. On days 0 and 4 after receiving the donor SW<sub>HEL</sub> B cells, the recipient mice were immunised with SRBCs that had been covalently decorated with HEL<sup>3X</sup>, a triply mutant HEL protein that binds with low affinity to HyHEL10 on the SW<sub>HEL</sub> B

cells.<sup>25,26</sup> Flow cytometric analysis of the spleen on day 15 revealed total GC B-cell numbers to be equivalent in recipients of LRBA-deficient or WT SW<sub>HEL</sub> B cells (Figure 6a). Unexpectedly, given the human phenotype of defective B-cell responses, we found a slight but significant increase in the total number of donor-derived, antigen-specific SW<sub>HEL</sub> GC B cells when these cells lacked LRBA (Figure 6b). In other respects, there was no significant difference between WT and LRBA-deficient SW<sub>HEL</sub> GC B cells in the fraction that bound low concentrations of HEL<sup>3X</sup> antigen (Figure 6c), had switched to IgG1 (Figure 6d) or exhibited a CD86<sup>+</sup> CXCR4<sup>-</sup> light-zone phenotype (Figure 6e). The mean CD86 on the donor-derived SW<sub>HEL</sub> GC B cells was also equivalent in the two groups (Figure 6f).

To investigate affinity maturation of LRBA-deficient cells in more detail, donor-derived SW<sub>HEL</sub> GC B cells from both groups of mice were individually sorted and the Hy10 VDJ<sub>H</sub> exon sequenced. There was a slight but significant increase in the mean number of amino-acid substitutions per cell in LRBA-deficient GC cells with no corresponding increase in silent nucleotide changes (Figure 6g). The pattern of amino-acid substitutions was equivalent between the two groups, including comparable percentages of cells that had acquired known HEL<sup>3X</sup> affinity-increasing mutations<sup>27</sup> (Figures 6h–j). Thus, LRBA-deficient B cells have no discernible deficit in T-cell-dependent activation, GC accumulation, isotype switching or affinity maturation when transplanted into mice with normal LRBA.

#### Recruitment and maintenance within the GC is normally controlled in LRBA-deficient mice despite abnormalities in CD86 expression

We extended the GC studies by performing reciprocal experiments where small numbers of *Lrba*<sup>+/+</sup> SW<sub>HEL</sub> B cells were injected into LRBA-deficient recipient mice so that the cooperating T cells would lack LRBA and have low CTLA-4. The 30 000 CD45.1-marked *Rag1*<sup>-/-</sup> SW<sub>HEL</sub> B cells were injected into *Lrba*<sup>-/-</sup> or *Lrba*<sup>+/+</sup> C57BL6 mice, the mice were immunised with HEL<sup>3X</sup>-SRBC on days 0 and 4, and spleen cells were analysed by flow cytometry on day 15. LRBA-deficient recipients exhibited no significant difference in the number of total GC B cells (Figure 7a), donor-derived SW<sub>HEL</sub> GC B cells (Figure 7b), recipient-derived GC B cells (Supplementary Figure 5A), nor in the proportion of donor or recipient-derived GC B cells that had switched to IgG1 (Figure 7c and Supplementary Fig 5B).

While LRBA-deficient recipients had normal GC B-cell numbers, cell surface CD86 was significantly increased on their total, non-GC (FAS<sup>lo</sup> CD38<sup>hi</sup>) B-cell population (Figure 7d). By contrast, CD86 was significantly decreased on donor- or recipient-derived GC B cells in LRBA-deficient mice (Figure 7e and Supplementary Figure 5C). CD86 was equally decreased when measured selectively on the light-zone

**Figure 4** Cell-autonomous loss of CTLA-4 on LRBA-deficient T cells in bone marrow chimeras. Irradiated *Rag1*<sup>-/-</sup> recipient mice were transplanted with a bone marrow mixture comprising 50% CD45.1<sup>+</sup> *Lrba*<sup>+/+</sup> cells and 50% CD45.2<sup>+</sup> cells that were either *Lrba*<sup>-/-</sup> or *Lrba*<sup>+/+</sup> (WT). One hundred percent CD45.2<sup>+</sup> *Lrba*<sup>-/-</sup> or *Lrba*<sup>+/+</sup> (WT) marrow was transplanted into a parallel group of *Rag1*<sup>-/-</sup> recipients. At 8 weeks after transplantation, the chimeric mice were immunised with SRBCs three times 3 days apart and blood was analysed by flow cytometry 62 days after the first immunisation. Lines connect paired values for CD45.1 and CD45.2 cells in individual chimeric mice. (a) Percentage of CD45.2<sup>+</sup> *Lrba*<sup>-/-</sup> (blue) or *Lrba*<sup>+/+</sup> (WT, red) cells among the indicated lymphocyte subsets in individual mixed chimeric mice and arithmetic means: B cells (B220<sup>+</sup>), T cells (CD3<sup>+</sup>), CD4<sup>+</sup> T cells, effector CD4<sup>+</sup> T cells (CD25<sup>+</sup>, CD44<sup>hi</sup>), CD8<sup>+</sup> T cells, effector CD8<sup>+</sup> T cells (CD25<sup>+</sup>, CD44<sup>hi</sup>) and Tregs (CD4<sup>+</sup>FOXP3<sup>+</sup>). (b–e) Analysis of CD4<sup>+</sup> FOXP3<sup>-</sup> cells. (b) Representative plots of intracellular CTLA-4 and CD44 gated on CD45.1<sup>+</sup> (WT) or CD45.2<sup>+</sup> (WT or *Lrba*<sup>-/-</sup>) CD4<sup>+</sup> FOXP3<sup>-</sup> cells. (c–e) Analysis of CTLA4<sup>+</sup> CD44<sup>+</sup> CD4<sup>+</sup> FOXP3<sup>-</sup> cells, showing: (c) percentage among the CD45.1<sup>+</sup> or CD45.2<sup>+</sup> subsets of total T cells; (d) representative CTLA-4 histograms; (e) CTLA-4 MFI values. Dotted lines represent CD45.2<sup>+</sup> (*Lrba*<sup>+/+</sup> or *Lrba*<sup>-/-</sup>) cells in mixed chimeras; solid lines represent equivalent cells in 100% *Lrba*<sup>+/+</sup> or *Lrba*<sup>-/-</sup> chimeras. (f–j) Analysis of CD4<sup>+</sup> FOXP3<sup>+</sup> cells. (f) Representative flow cytometric plots of CD45.2<sup>+</sup> CD4<sup>+</sup> cells, showing % Tregs. (g) CTLA-4 MFI values for each chimeric mouse. (h) Representative intracellular CTLA-4 histograms. (i) Representative intracellular FOXP3 histograms. (j) Representative CD25 histograms. Statistical analysis was carried out using *t*-test between mice or paired *t*-test when cells were from the same chimeric mouse: \**P*<0.05; \*\**P*<0.01; \*\*\**P*<0.001; \*\*\*\**P*<0.0001. *N*=5 per group. Data are representative of one experiment.

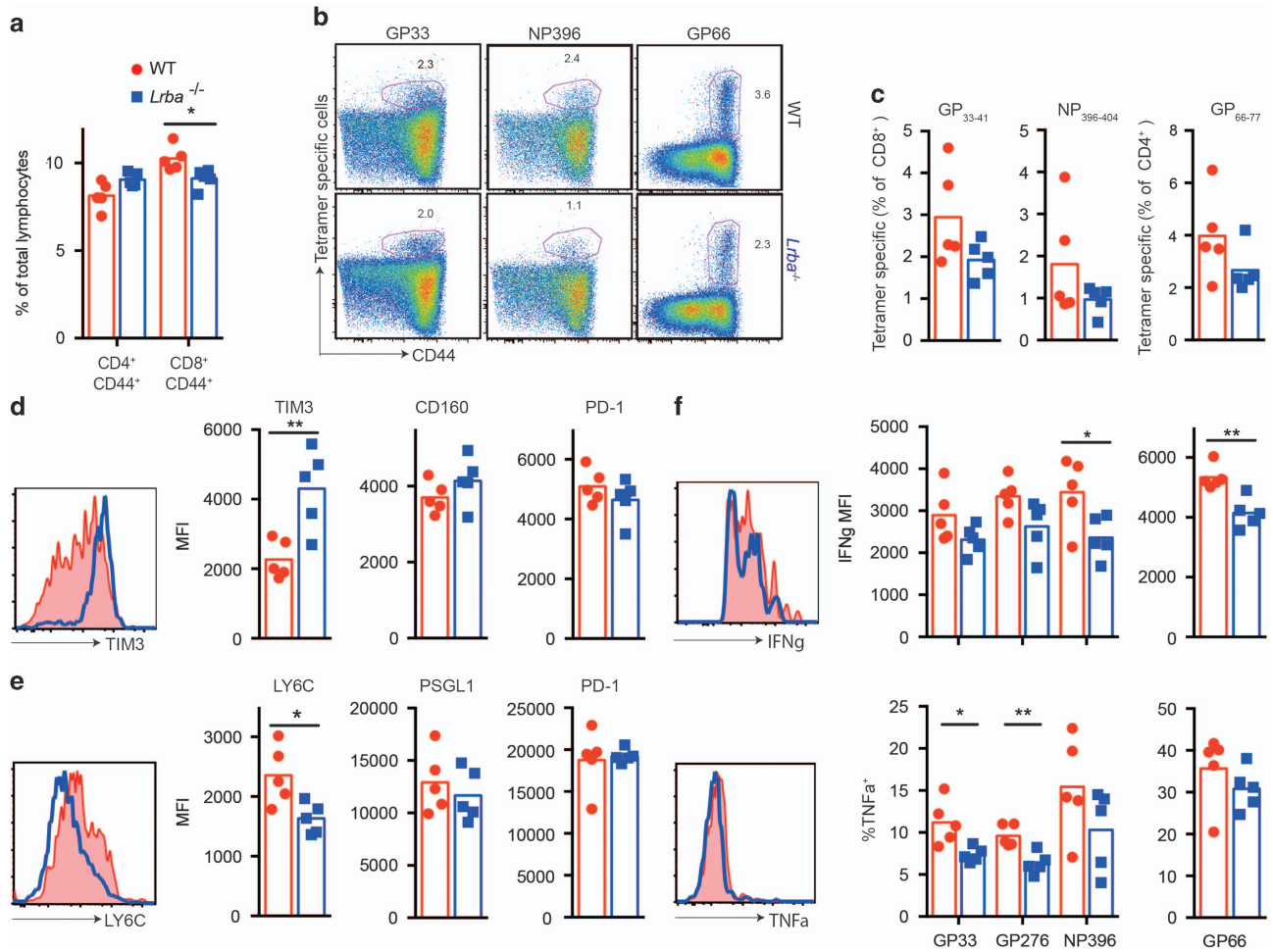


**Figure 5** Response of LRBA-deficient mice to chronic systemic viral infection. C57BL/6 *Lrba*<sup>+/+</sup> (WT) (red) or *Lrba*<sup>-/-</sup> mice (blue) were infected intravenously with  $2 \times 10^6$  plaque-forming unit (PFU) LCMV clone 13 to induce chronic viral infection. At 20 days after infection, spleen cells were analysed by flow cytometry. (a) Analysis plots of spleens, showing % of lymphocytes that are CD44<sup>hi</sup> effector/memory cells in individual mice with arithmetic means. (b and c) Representative flow cytometric plots (b) and analysis plots (c) showing % of CD8<sup>+</sup> T cells binding MHC I tetramers loaded with LCMV peptides GP<sub>33-41</sub> or NP<sub>396-404</sub>, or the % of CD4<sup>+</sup> cells binding MHC II tetramers fused with LCMV peptide GP<sub>66-77</sub> in individual mice with arithmetic means. (d) Representative histograms showing TIM3 staining on NP<sub>396-404</sub> MHC I tetramer-binding CD8<sup>+</sup> T cells in WT and *Lrba*<sup>-/-</sup> mice, and MFIs in individual animals for TIM3, CD160 and PD-1. Similar trends were seen with the GP<sub>33-41</sub> tetramer. (e) Representative LY6C staining on GP<sub>66-77</sub> MHC II tetramer-binding CD4<sup>+</sup> T cells, and MFIs in individual animals for LY6C, PSGL1 and PD-1. (f) IFN $\gamma$ <sup>+</sup> MFI of the IFN $\gamma$ <sup>+</sup> T cells (top) and % TNF $\alpha$ <sup>+</sup> within the IFN $\gamma$ <sup>+</sup> cells. Representative IFN $\gamma$  and TNF $\alpha$  histograms are shown for the NP396 peptide-stimulated cells. Statistical analysis was carried out using *t*-test: \**P* < 0.05; \*\**P* < 0.01. *N* = 5 per group. Data are representative of one experiment. IFN $\gamma$ , interferon- $\gamma$ .

subset of GC B cells (Figures 7f and g and Supplementary Figures 5D and E). Lower CD86 on SW<sub>HEL</sub> GC B cells in *Lrba*<sup>-/-</sup> recipients nevertheless did not translate into any discernable change in affinity maturation. When these GC B cells were individually sorted and their *VDJ<sub>H</sub>* exon sequenced, there were comparable frequencies of total and affinity-increasing mutations in *Lrba*<sup>-/-</sup> or *Lrba*<sup>+/+</sup> recipient mice (Figures 7i-l).

**DISCUSSION**

The experiments here add to the experimental evidence base for treating LRBA deficiency with CTLA4-Ig (Abatacept), and pose questions about the limitations of laboratory experiments in mice to reproduce human disease *in natura*. We show that LRBA has a critical, cell-autonomous role promoting CTLA-4 accumulation within CD4 effector T cells and Tregs in otherwise healthy mice. Despite the lower CTLA-4, acute experimental challenge of LRBA-deficient mice failed to reproduce the severe immune dysregulation that develops in LRBA-

deficient children. In young mice, or in chimeric mice where only half of the T cells are LRBA-deficient, low CTLA-4 was the only detectable abnormality in Tregs. Other abnormalities described in Tregs from LRBA-deficient patients, notably low FOXP3 and CD25, were only observed in 6-month-old LRBA-deficient mice and were not apparent in mixed chimeras, raising the possibility that they arise by gradual Treg 'exhaustion' as a secondary consequence of insufficient CTLA-4. Evidence that low Treg expression of FOXP3 and CD25 arises as a secondary consequence of insufficient CTLA-4 comes from patients with heterozygous CTLA-4 loss-of-function mutations, who display these Treg abnormalities when they are ill with morbid immune dysregulation but not in healthy relatives carrying the same CTLA-4 mutation.<sup>28,29</sup> The lower frequencies of Tregs in LRBA-deficient patients may also result from Treg exhaustion after chronic overstimulation by successive infections *in natura*. We observed no significant decrease in Treg numbers in 6-month-old LRBA-deficient mice housed in a specific pathogen-free environment, and no

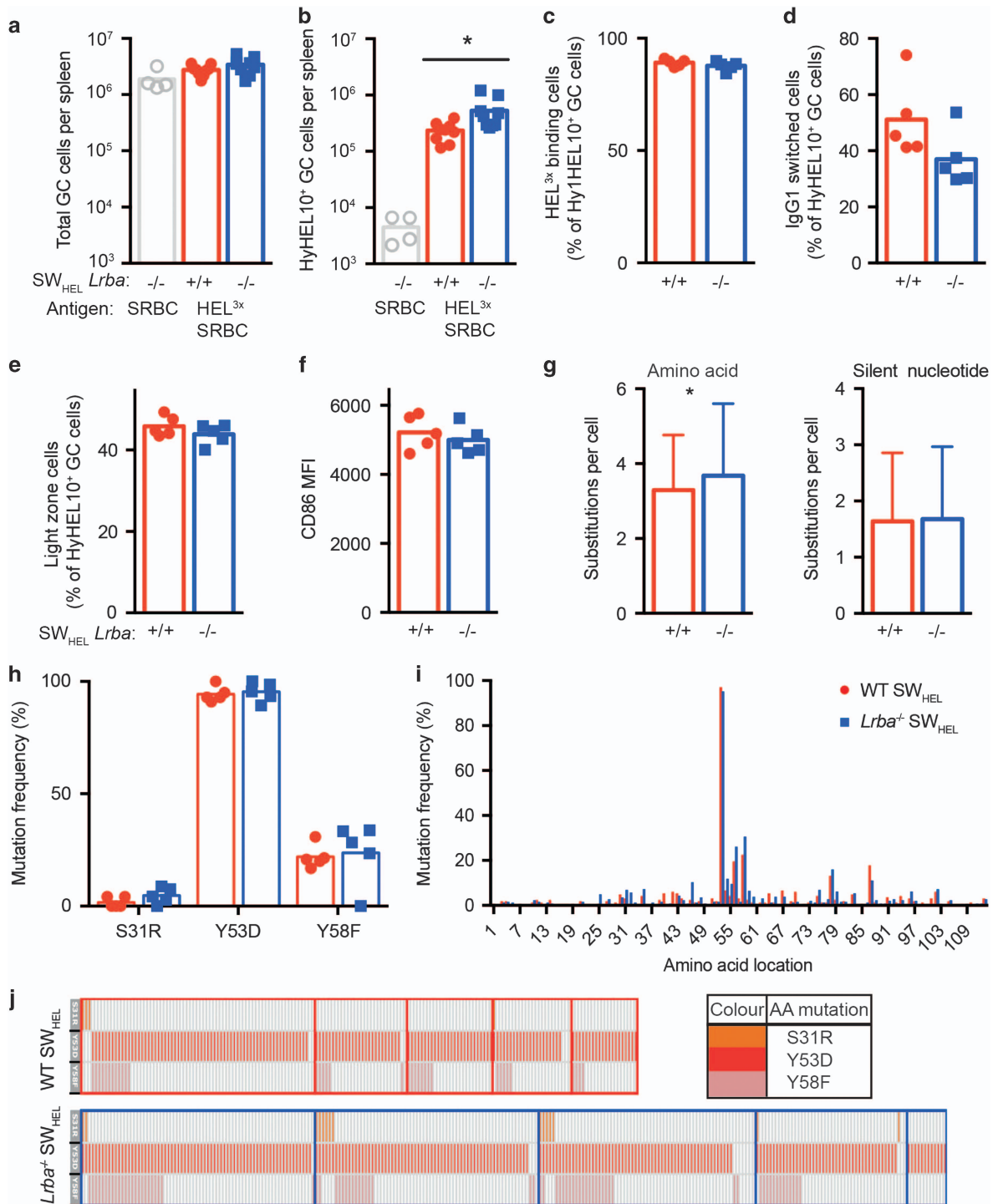
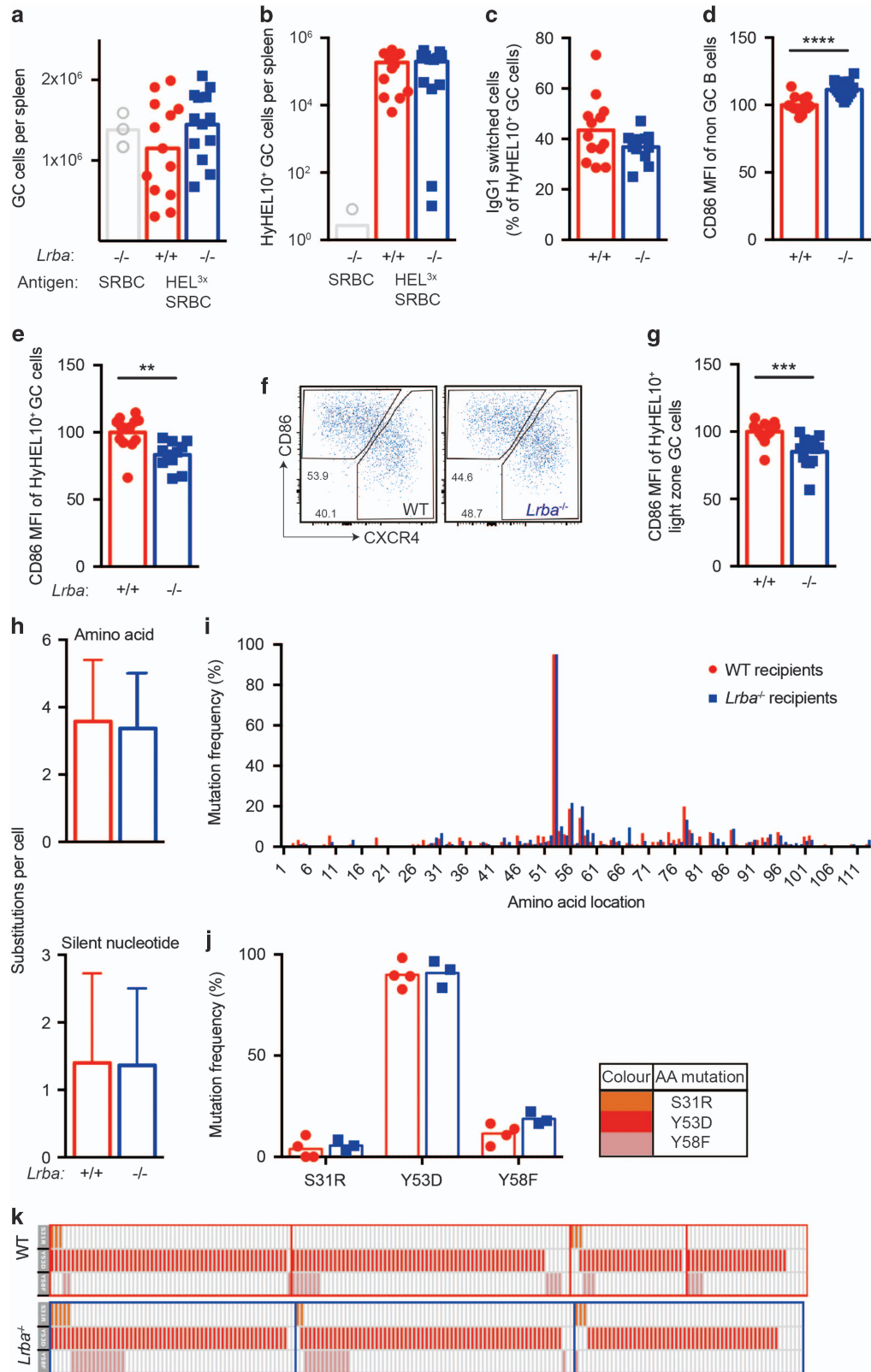


**Figure 6** Normal GC formation and affinity maturation by LRBA-deficient B cells. CD45.1 congenic C57BL/6 recipient mice, with WT LRBA, were injected intravenously with 30 000 HyHEL10<sup>+</sup> SW<sub>HEL</sub> spleen B cells from *Lrba*<sup>-/-</sup> or *Lrba*<sup>+/+</sup> C57BL/6 donor mice. The recipient mice were immunised two times on days 0 and 4 after B-cell transfer with HEL<sup>3x</sup>-SRBC, or unconjugated SRBC for a control group of recipients, and spleen cells were analysed by flow cytometry, sorting and single-cell *Igh* sequencing on day 15. (a) Total Fas<sup>hi</sup> CD38<sup>-</sup> B220<sup>+</sup> GC B cells per spleen of individual mice, and arithmetic mean for each group. (b) Donor-derived HyHEL10<sup>+</sup> CD45.2<sup>+</sup> CD45.1<sup>-</sup> GC B cells per spleen. (c) Affinity-matured cells, measured as % donor-derived GC B cells stained brightly with 200 ng/ml HEL<sup>3x</sup>. (d) IgG1-switched cells, measured as % of donor-derived GC B cells. (e) Light-zone CD86<sup>+</sup> CXCR4<sup>-</sup> GC B cells, measured as % of donor-derived GC B cells. (f) CD86 MFI on donor-derived GC B cells. (g) Number of *VDJ<sub>H</sub>* amino-acid changing or silent nucleotide substitutions per donor-derived GC B cell. (h) Percentage of donor-derived GC B cells with affinity-increasing *VDJ<sub>H</sub>* mutations S31R, Y53D or Y58F. (i) Percentage of donor-derived GC B cells with substitutions at each *VDJ<sub>H</sub>* amino-acid position. (j) Co-occurrence of S31R, Y53D and Y58F mutations (rows) in individual cells (columns) sorted from separate recipient mice (boxes). Data are pooled from two independent experiments with comparable results. *N*=9 mice per HEL<sup>3x</sup>-immunised group and four unconjugated controls. Statistical analysis was carried out using *t*-test: \**P*<0.05.



competitive disadvantage for accumulation of LRBA-deficient Tregs in mixed chimeras. Future studies will need to determine if the limitations of the mouse model stem from subtle differences in species sensitivity to partial CTLA-4 deficiency, different functions of

LRBA in humans and mice, the need for an autoimmune-predisposed genetic background or the need for particular environmental triggers.

While the CTLA-4 results are consistent in mice and humans,<sup>11</sup> the experiments here provide no evidence that LRBA is required within B

cells. In contrast to the hypogammaglobulinemia that characterises human LRBA deficiency, especially affecting IgA, LRBA-deficient mice had normal serum IgG1 and IgM, significantly increased levels of serum IgG2b and a trend towards increased IgA. Since the latter two isotypes are induced by tumour growth factor- $\beta$ ,<sup>30</sup> it will be interesting in future studies to explore the possibility that the low CTLA4 on helper T cells or Tregs results in higher expression of tumour growth factor- $\beta$ .

By transferring small numbers of LRBA-deficient or WT SW<sub>HEL</sub> B cells into WT recipients, we observed the deficient B cells accumulated to slightly higher GC numbers and had no deficit in isotype switching or affinity maturation. A theoretical limitation of this model is that the antigen-specific B cells start at a frequency of  $\sim 1$  in 10 000 B cells, which may be higher than some antigen-specific precursors in the normal response. Nevertheless, the same assay reveals a profound deficit caused by DOCK8 deficiency, which also causes common variable immunodeficiency in humans.<sup>31</sup> The normal GC B-cell responses by LRBA-deficient B cells may either represent a human-mouse difference, or the deficiency of switched memory B cells in LRBA-deficient patients may be secondary to their severe immune dysregulation brought about by CTLA-4 deficiency. Support for the latter conclusion comes from patients with heterozygous *CTLA4* loss-of-function mutations: despite *CTLA4* mRNA being exclusively expressed in T cells and not B cells, these patients have a progressive decrease in B cells and switched memory B cells, hypogammaglobulinemia and recurrent respiratory infections as part of a similar immune dysregulation syndrome.<sup>28,29</sup>

The one B-cell abnormality observed in LRBA-deficient mice was a relative decrease in the B-1 B-cell subset in the peritoneal cavity of young and aged mice. B-1 cells express a BCR repertoire that is polyspecific and crossreactive for both self and microbial antigens.<sup>32</sup> In this way, these cells have an important role in maintaining tissue homeostasis, and innate-like immune defence against mucosal pathogens.<sup>32,33</sup> In addition, B-1 cells produce interleukin-10 and have important roles in the maintenance of self-tolerance by the uptake and presentation of endogenous antigens.<sup>34,35</sup> B-1 cells have also been linked to autoimmunity in both human patients and murine models of disease.<sup>36</sup> We found that the T-cell compartment of the peritoneal fluid was also increased relatively to the other cell types in the sample in LRBA-deficient mice. These peritoneal cell abnormalities are peculiar given that, to our knowledge, there is no reported link between CTLA-4 and B-1 cell production. Future experiments will be needed to resolve whether the peritoneal cavity abnormalities reflect a primary role for LRBA within the B-1 or T cells in that site, or a secondary reaction to primary abnormalities in the LRBA-deficient gut, as *LRBA* mRNA is particularly abundant in the intestine.

The key question arising from our findings is why low CTLA-4 in LRBA-deficient mice does not result in morbid immune dysregulation

with accumulation of effector T cells and splenomegaly/lymphadenopathy, as observed in the majority of humans with LRBA deficiency where it responds to CTLA4-Ig therapy.<sup>4-17</sup> In patients, the clinical syndrome can take up to 10 years to present,<sup>6,18</sup> raising the possibility that it requires an environmental trigger. However, when we challenged LRBA-deficient mice with two short-term interventions that are powerful triggers of innate and adaptive immunity, repeated SRBC injections or chronic systemic LCMV infection, neither triggered discernable immune dysregulation. It is conceivable that dysregulation might develop following immune stimulation over a much longer time frame or potentially require a genetic background more prone to autoimmunity than C57BL/6 mice, and this could be explored in the future.

A similar discordance between humans and mice exists for the clinical manifestations of heterozygous CTLA-4 deficiency. Humans with heterozygous mutations that decrease *CTLA4* mRNA by 50% or decrease CTLA-4 protein by a similar amount develop an immune dysregulation syndrome with common variable immunodeficiency and autoimmunity that resembles LRBA deficiency, albeit also after a variable latent phase and with clear evidence of incomplete penetrance.<sup>28,29</sup> CTLA-4 has a similar role in humans and mice, because homozygous null *CTLA4* mutations in mice result in fatal lymphoproliferative disease within weeks after birth,<sup>21,22</sup> and complete deletion of *CTLA4* in adult mice results in lymphoproliferation, especially of the Treg compartment, expanded GCs, hypergammaglobulinemia and organ-specific autoantibodies.<sup>21,37,38</sup> However, laboratory mice with heterozygous null *Ctla4* mutations are phenotypically normal.<sup>21,28</sup>

Our analysis together with published findings suggests that several mechanisms may allow LRBA-deficient or *CTLA4* heterozygous mice to compensate for decreased CTLA-4 in Treg and effector T cells. CD86 is normally removed from the surface of B cells and other antigen-presenting cells by CTLA-4 on Tregs and effector T cells.<sup>19</sup> The finding here that CD86 was not increased on marginal zone and follicular B cells of unimmunised LRBA-deficient mice despite lower CTLA-4 on Tregs and effector T cells may simply reflect mass action: the low rate of CD86 production on unstimulated B cells may result in sufficient CTLA-4 even when decreased to 30% of normal. In immunised mice, increased CD86 on total (non-GC) B cells was previously observed when CTLA-4 deficiency was induced acutely in Tregs.<sup>38,39</sup> Interestingly, CD86 levels were not elevated on GC B cells in the same mice in one study.<sup>39</sup> Here, we also found that immunised LRBA-deficient mice displayed increased CD86 on non-GC B cells, but decreased CD86 on GC B cells. Collectively, the results here and in Sage *et al.*<sup>39</sup> imply that compensatory mechanisms can attenuate CD86 selectively on GC B cells when there is insufficient CTLA-4 to regulate CD86 on B cells outside the GC. Compensation could arise from the higher concentration of Tregs in the GC, and the ability of LRBA-

**Figure 7** Normal GC formation and affinity maturation by LRBA WT B cells in LRBA-deficient recipients. The 30 000 HyHEL10<sup>+</sup> SW<sub>HEL</sub> B cells from *Rag1*<sup>-/-</sup> CD45.1 congenic mice, with WT LRBA, were injected into the circulation of *Lrba*<sup>-/-</sup> ( $n=13$ , blue symbols) or *Lrba*<sup>+/+</sup> ( $n=13$ , red symbols) C57BL/6 recipient mice, so that all T- and B-cell specificities other than the HyHEL10<sup>+</sup> B cells were derived from the recipient mice. The recipient mice were immunised two times with HEL<sup>3X</sup>-SRBC on days 0 and 4 after B-cell transfer, or unconjugated SRBC for a control group of recipients, and spleen cells analysed by flow cytometry, sorting and single-cell *Igh* sequencing on day 15. (a) Total Fas<sup>hi</sup> CD38<sup>-</sup> B220<sup>+</sup> GC B cells per spleen of individual mice, and arithmetic mean for each group. (b) Donor-derived HyHEL10<sup>+</sup> CD45.2<sup>-</sup> CD45.1<sup>+</sup> GC B cells per spleen. (c) IgG1-switched cells, measured as % of donor-derived GC B cells. (d and e) Relative cell surface of CD86 MFI on (d) all B220<sup>+</sup> B cells or (e) donor-derived GC B cells, normalised to mean of *Lrba*<sup>+/+</sup> recipient group in each experiment. (f) Representative plots of donor-derived GC B cells, and gates on light-zone (LZ, CD86<sup>hi</sup> CXCR4<sup>lo</sup>) and dark-zone (CD86<sup>lo</sup> CXCR4<sup>hi</sup>) GC cells. (g) Relative cell surface CD86 MFI on LZ donor-derived GC B cells, normalised to mean of *Lrba*<sup>+/+</sup> recipient group in each experiment. (h) Number of *VDJ<sub>H</sub>* amino-acid changing or silent nucleotide substitutions per donor-derived GC B cell. (i) Percentage of donor-derived GC B cells with substitutions at each *VDJ<sub>H</sub>* amino-acid position. (j) Percentage of donor-derived GC B cells with affinity-increasing *VDJ<sub>H</sub>* mutations S31R, Y53D or Y58F. (k) Co-occurrence of S31R, Y53D and Y58F mutations (rows) in individual cells (columns) sorted from separate recipient mice (boxes). Data are pooled from two independent experiments with comparable results. Statistical analysis was carried out using *t*-test: \*\* $P<0.01$ ; \*\*\* $P<0.001$ .

deficient Tregs to increase CTLA-4 upon stimulation.<sup>40</sup> As a complementary pathway, CTLA-4-deficient Tregs increase interleukin-10 production,<sup>41</sup> a cytokine that induces *March1* in GC B cells to ubiquitinate and degrade CD86.<sup>42–44</sup> The finding of elevated TIM3 on virus-reactive CD8 cells raises the possibility of other compensating inhibitory feedback mechanisms in effector T cells, as TIM3 along with TIGIT is a parallel T-cell inhibitory receptor to CTLA-4. These hypothetical compensating mechanisms for controlling CD86 and T-cell costimulation are beyond the scope of this study and will require investigation in the future.

In summary, we have shown that LRBA deficiency in mice results in biochemical defects of low CTLA-4 in activated CD4<sup>+</sup> T cells and Tregs that are comparable to those seen in patients, yet decreased CTLA-4 alone is sufficient only to induce subclinical abnormalities in laboratory mice. This primary, selective CTLA-4 deficiency adds to the experimental rationale for treating LRBA-deficient patients with CTLA4-Ig as a replacement therapy. Aged LRBA-deficient mice showed downregulation of other proteins in Tregs including FOXP3 and CD25, mimicking that seen in patients. Progression from these subclinical abnormalities to clinical immune dysregulation may reflect a broadening of Treg abnormalities to disrupt other compensatory mechanisms for dampening CD86 expression on B cells and other antigen-presenting cells.

## METHODS

### Mice

All mice used in the experiments were bred at Australian BioResources (Moss Vale, NSW, Australia) and held at the Garvan Institute of Medical Research in specific pathogen-free environments. The Garvan Animal Ethics Committee approved all mice protocols and procedures.

C57BL/6 (WT) mice were purchased from the Australian BioResources. To generate *lrba*<sup>-/-</sup> mice, a single-guide RNA with the sequence 5'-TTAACTGAGTTGCGGTCACATGG-3' (PAM underlined) was microinjected together with Cas9 mRNA into C57BL/6 zygotes. Four of the resulting founder mice were homozygous for an 8 bp deletion eliminating Chr3:86445 392–86 445 399 (Build GRCm38) in exon 37 of the LRBA allele.

HyHEL10-transgenic (SW<sub>HEL</sub>) mice have been described previously.<sup>45</sup> These mice carry a single-copy V<sub>H</sub>10 anti-HEL heavy-chain variable region coding exon targeted to the endogenous IgH allele plus multiple copies of V<sub>H</sub>10-κ anti-HEL light-chain transgene. SW<sub>HEL</sub> mice were maintained on a CD45.1 congenic (*Ptprc<sup>ca</sup>*) C57BL6 background. For experiments where SW<sub>HEL</sub> cells were transferred into LRBA-deficient mice, SW<sub>HEL</sub> mice were crossed with *Rag1*-knockout mice<sup>46</sup> to prevent endogenous *Igh* or *Igk* gene rearrangement, so that all the developing B cells expressed HyHEL10. This ensured that no *lrba*<sup>+/+</sup> T cells were transferred into LRBA-deficient mice for these experiments.

In addition, SW<sub>HEL</sub> mice were crossed with *lrba*<sup>-/-</sup> mice to generate HyHEL10-transgenic B cells lacking LRBA.

For all experimental interventions animals of both sexes were used in each experimental group and matched for numbers of males and females in test and control groups. Animals were excluded if before recruitment they showed any clinical abnormalities on routine physical examination.

### Bone marrow chimeras and SRBC immunisation

Recipient C57BL/6 *Rag1*<sup>-/-</sup> mice 8–12 weeks old were irradiated with 425 cGy using an X-RAD 320 Biological Irradiator (Precision X-Ray). Donor bone marrow was aspirated from femurs, humeri and tibia into B-cell medium comprising RPMI (Gibco) with 10% heat-inactivated foetal calf serum (Gibco), 2 mM L-glutamine and 100 U/ml penicillin RPMI media (Gibco). At 15 h after irradiation, recipient mice were transplanted with an intravenous injection of 5–10 × 10<sup>6</sup> bone marrow cells, comprising a mixture of 50% from CD45.1 congenic C57BL/6 mice and 50% from C57BL6 (CD45.2) mice that were either *lrba*<sup>-/-</sup> or *lrba*<sup>+/+</sup>.

Unmanipulated mice 8 weeks old, and bone marrow chimeras 8 weeks after marrow transplantation, were immunised with 2 × 10<sup>8</sup> SRBCs given intravenously.

### Recombinant HEL proteins

Recombinant HEL<sup>3X</sup> were made as secreted proteins in *Pichia pastoris* yeast (Invitrogen) and purified from culture supernatants by ion exchange chromatography as described previously.<sup>26,27,45</sup> Proteins were stored in phosphate-buffered saline at 1–2.5 mg ml<sup>-1</sup> at -80 °C. Before use samples were thawed and stored at 4 °C for a maximum of 8 months. Upon thawing, protein concentrations were determined by spectrophotometry at 280 nm.

### SRBC conjugation and transfer

HEL proteins were desalted into Conjugation buffer (distilled water with 0.35 M D-mannitol (Sigma) and 0.01 M sodium chloride (Sigma)). For this process, PD-10 columns (Amersham) were equilibrated with 30 ml Conjugation buffer. One hundred micrograms of protein was loaded onto each column and pushed through the column using 2.5 ml Conjugation buffer. For elution of the protein 3.5 ml Conjugation buffer was added and the HEL protein was collected as fractions in the following volumes: 250, 1000, 250, 250 and 250 μl. Protein concentrations of each fraction were determined by spectrophotometry.

For conjugation, SRBCs were washed in 30 ml of phosphate-buffered saline per 6–8 × 10<sup>9</sup> cells and then once in the Conjugation buffer. SRBCs were then resuspended in a final volume of 1000 μl conjugation buffer in a 50 ml Falcon tube containing 10 μg ml<sup>-1</sup> of HEL<sup>3X</sup>. The solution was mixed on a platform rocker on ice for 10 min. One hundred microliters of 100 mg ml<sup>-1</sup> N-(3-dimethylaminopropyl)-N-ethylcarbodiimide hydrochloride (Sigma) was then added and the solution was mixed for a further 30 min on ice. Confirmation of successful conjugation was performed by flow cytometric analysis of SRBC using AlexaFluor 647-conjugated HyHEL9 antibody (generated in-house).

Intravenous transfers of 3 × 10<sup>4</sup> SW<sub>HEL</sub> B cells per recipient mouse together with 2 × 10<sup>8</sup> HEL<sup>3X</sup> SRBC as described previously.<sup>26</sup>

### Haematology and flow cytometry

Red blood cells and platelet numbers were determined in blood collected from the tail-vein into EDTA (Sarstedt) tubes and analysed on a Sysmex XT-2000iV automated haematology analyser.

On the day of harvest organs were collected into B-cell medium, cell suspensions passed through a 70 μm cell strainer (Falcon). Fc receptors were blocked with unlabelled anti-CD16/32 (eBioscience) before staining. To detect HEL<sup>3X</sup>-binding cells, cells were stained with 200 ng ml<sup>-1</sup> HEL<sup>3X</sup>, followed by AlexaFluor 647-conjugated HyHEL9.

Anti-IgG1-FITC (BD) stains were followed by 5% mouse serum before staining for other surface molecules. CD4-BV786 (BD), CD8-APCCy7 (BD), CD62L-PerCPCy5.5 (BD) CD44-FITC (BD) and CD25-PE (BD) were used as surface stains. For the intracellular stains, CTLA-4-APC (eBioscience) and FOXP3-EF450 (eBioscience) cells were first permeabilised using FOXP3 Staining Permeabilisation Kit (eBioscience) according to the manufacturer's instructions. Cells were filtered using 35 μm filter round-bottom FACS tubes (BD) immediately before data acquisition on an LSR II analyser (BD).

Cytometer files were analysed with the FlowJo Software (TreeStar).

### Single-cell FACS sorting

Cell suspensions were prepared and GC B cells were identified using flow cytometry. Single-cell sorting into 96-well plates (Thermo Fisher Scientific) was performed on the FACSaria or FACSariaIII (BD). B cells from each mouse were analysed individually to ensure that over-representation of one particular clone did not affect the mutation analysis. The *VDJ<sub>H</sub>* exon of the Hy10 heavy-chain gene was amplified from genomic DNA by PCR, sequenced and analysed as described previously.<sup>27</sup>

### Enzyme-linked immunosorbent assay

High-binding plates (Corning) were coated with the indicated Ig isotypes at 5 μg ml<sup>-1</sup> (IgG2b (BD), clone: R9-91; IgA (BD), clone: C10-3; IgG1 (BD), clone: A85-1; IgM (BD), clone: 11/41; IgG3 (BD), clone: R2-38; IgG2a(b) (BD),

clone: R11-89; IgE (BD), clone: R35-72). Bound serum antibody was quantified using Igk (BD). Antibody levels were quantified against isotype-specific standards (IgG2b BD, IgA BD, IgG1 BD, IgM BD, IgG3 BD, IgG2a(b) (Southern Biotech) and IgE (BioLegend)).

### Viral infection

Mice were infected intravenously with  $2 \times 10^6$  plaque-forming units of LCMV clone 13. T-cell stimulation with LCMV peptide, tetramer staining, surface staining and intracellular cytokine staining were performed as described previously.<sup>47–49</sup> MHC I LCMV tetramers were purchased from the Biomolecular Resource Facility, JCSMR, ANU, while the MHC II LCMV GP<sub>66–77</sub> tetramer was obtained from the NIH Tetramer Core Facility (Emory University, Atlanta, GA, USA).

### Statistical analysis

GraphPad Prism 6 (GraphPad Software, San Diego, CA, USA) was used for data analysis. When the data were normally distributed, two-tailed Student's *t*-test was performed for analysis. Welch's correction was used if variances were not equal. For all tests  $P < 0.05$  was considered as being statistically significant. In all graphs presented error bars indicate mean and standard distribution. \* $P < 0.05$ , \*\* $P < 0.01$ , \*\*\* $P < 0.001$  and \*\*\*\* $P < 0.0001$ .

### CONFLICT OF INTEREST

The authors declare no conflict of interest.

### ACKNOWLEDGEMENTS

We thank the Garvan Institute ABR, GMG and Flow Cytometry facilities for expert animal husbandry, genotyping and cell sorting. This work was supported by NHMRC Project Grant 1108800, NHMRC Program Grants 1016953 and 1113904, NIH Grant U19 AI1100627 and NHMRC Fellowship 1081858, and by the Ritchie Family Foundation.

- Cullinane AR, Schaffer AA, Huizing M. The BEACH is hot: a LYST of emerging roles for BEACH-domain containing proteins in human disease. *Traffic* 2013; **14**: 749–766.
- Feuchter AE, Freeman JD, Mager DL. Strategy for detecting cellular transcripts promoted by human endogenous long terminal repeats: identification of a novel gene (CDC4L) with homology to yeast CDC4. *Genomics* 1992; **13**: 1237–1246.
- Wang JW, Howson J, Haller E, Kerr WG. Identification of a novel lipopolysaccharide-inducible gene with key features of both A kinase anchor proteins and chs1/beige proteins. *J Immunol* 2001; **166**: 4586–4595.
- Lopez-Herrera G, Tampella G, Pan-Hammarstrom Q, Herholz P, Trujillo-Vargas CM, Phadwal K *et al*. Deleterious mutations in LRBA are associated with a syndrome of immune deficiency and autoimmunity. *Am J Hum Genet* 2012; **90**: 986–1001.
- Alangari A, Alsultan A, Adly N, Massaad MJ, Kiani IS, Aljebreen A *et al*. LPS-responsive beige-like anchor (LRBA) gene mutation in a family with inflammatory bowel disease and combined immunodeficiency. *J Allergy Clin Immunol* 2012; **130**: 481–8 e2.
- Alkhairy OK, Abolhassani H, Rezaei N, Fang M, Andersen KK, Chavoshzadeh Z *et al*. Spectrum of phenotypes associated with mutations in LRBA. *J Clin Immunol* 2016; **36**: 33–45.
- Burns SO, Zenner HL, Plagnol V, Curtis J, Mok K, Eisenhut M *et al*. LRBA gene deletion in a patient presenting with autoimmunity without hypogammaglobulinemia. *J Allergy Clin Immunol* 2012; **130**: 1428–1432.
- Charbonnier LM, Janssen E, Chou J, Ohsumi TK, Keles S, Hsu JT *et al*. Regulatory T-cell deficiency and immune dysregulation, polyendocrinopathy, enteropathy, X-linked-like disorder caused by loss-of-function mutations in LRBA. *J Allergy Clin Immunol* 2015; **135**: 217–227.
- Lee S, Moon JS, Lee CR, Kim HE, Baek SM, Hwang S *et al*. Abatacept alleviates severe autoimmune symptoms in a patient carrying a *de novo* variant in CTLA-4. *J Allergy Clin Immunol* 2016; **137**: 327–330.
- Levy E, Stolzenberg MC, Bruneau J, Breton S, Neven B, Sauvion S *et al*. LRBA deficiency with autoimmunity and early onset chronic erosive polyarthritis. *Clin Immunol* 2016; **168**: 88–93.
- Lo B, Zhang K, Lu W, Zheng L, Zhang Q, Kanellopoulou C *et al*. Autoimmune disease. Patients with LRBA deficiency show CTLA4 loss and immune dysregulation responsive to abatacept therapy. *Science* 2015; **349**: 436–440.
- Revel-Vilk S, Fischer U, Keller B, Nabhani S, Gamez-Diaz L, Rensing-Ehl A *et al*. Autoimmune lymphoproliferative syndrome-like disease in patients with LRBA mutation. *Clin Immunol* 2015; **159**: 84–92.
- Sari S, Dogu F, Hwa V, Haskoğlu S, Dauber A, Rosenfeld R *et al*. A successful HSCT in a girl with novel LRBA mutation with refractory celiac disease. *J Clin Immunol* 2016; **36**: 8–11.
- Schreiner F, Plamper M, Dueker G, Schoenberger S, Gamez-Diaz L, Grimbacher B *et al*. Infancy-onset T1DM, short stature, and severe immunodysregulation in two siblings with a homozygous LRBA mutation. *J Clin Endocrinol Metab* 2016; **101**: 898–904.
- Seidel MG, Hirschmugl T, Gamez-Diaz L, Schwinger W, Serwas N, Deutschmann A *et al*. Long-term remission after allogeneic hematopoietic stem cell transplantation in LPS-responsive beige-like anchor (LRBA) deficiency. *J Allergy Clin Immunol* 2015; **135**: 1384–90 e1-8.
- Serwas NK, Kansu A, Santos-Valente E, Kuloglu Z, Demir A, Yaman A *et al*. Atypical manifestation of LRBA deficiency with predominant IBD-like phenotype. *Inflamm Bowel Dis* 2015; **21**: 40–47.
- Tesi B, Priftakis P, Lindgren F, Chiang SC, Kartalis N, Lofstedt A *et al*. Successful hematopoietic stem cell transplantation in a patient with LPS-responsive beige-like anchor (LRBA) gene mutation. *J Clin Immunol* 2016; **36**: 480–489.
- Gamez-Diaz L, August D, Stepensky P, Revel-Vilk S, Seidel MG, Noriko M *et al*. The extended phenotype of LPS-responsive beige-like anchor protein (LRBA) deficiency. *J Allergy Clin Immunol* 2016; **137**: 223–230.
- Qureshi OS, Zheng Y, Nakamura K, Attridge K, Manzotti C, Schmidt EM *et al*. Trans-endocytosis of CD80 and CD86: a molecular basis for the cell-extrinsic function of CTLA-4. *Science* 2011; **332**: 600–603.
- Rathmell JC, Fournier S, Weintraub BC, Allison JP, Goodnow CC. Repression of B7.2 on self-reactive B cells is essential to prevent proliferation and allow Fas-mediated deletion by CD4<sup>+</sup> T cells. *J Exp Med* 1998; **188**: 651–659.
- Waterhouse P, Penninger JM, Timms E, Wakeham A, Shahinian A, Lee KP *et al*. Lymphoproliferative disorders with early lethality in mice deficient in Ctl4. *Science* 1995; **270**: 985–988.
- Tivol EA, Borriello F, Schweitzer AN, Lynch WP, Bluestone JA, Sharpe AH. Loss of Ctl4 leads to massive lymphoproliferation and fatal multiorgan tissue destruction, revealing a critical negative regulatory role of Ctl4. *Immunity* 1995; **3**: 541–547.
- Yi T, Li J, Chen H, Wu J, An J, Xu Y *et al*. Splenic dendritic cells survey red blood cells for missing self-CD47 to trigger adaptive immune responses. *Immunity* 2015; **43**: 764–775.
- Whery EJ, Ha SJ, Kaech SM, Haining WN, Sarkar S, Kalia V *et al*. Molecular signature of CD8<sup>+</sup> T cell exhaustion during chronic viral infection. *Immunity* 2007; **27**: 670–684.
- Phan TG, Paus D, Chan TD, Turner ML, Nutt SL, Basten A *et al*. High affinity germinal center B cells are actively selected into the plasma cell compartment. *J Exp Med* 2006; **203**: 2419–2424.
- Paus D, Phan TG, Chan TD, Gardam S, Basten A, Brink R. Antigen recognition strength regulates the choice between extrafollicular plasma cell and germinal B cell differentiation. *J Exp Med* 2006; **203**: 1081–1091.
- Chan TD, Wood K, Hermes JR, Butt D, Jolly CJ, Basten A *et al*. Elimination of germinal-center-derived self-reactive B cells is governed by the location and concentration of self-antigen. *Immunity* 2012; **37**: 893–904.
- Kuehn HS, Ouyang WM, Lo B, Deenick EK, Niemela JE, Avery DT *et al*. Immune dysregulation in human subjects with heterozygous germline mutations in CTLA4. *Science* 2014; **345**: 1623–1627.
- Schubert D, Bode C, Kenefeck R, Hou TZ, Wing JB, Kennedy A *et al*. Autosomal dominant immune dysregulation syndrome in humans with CTLA4 mutations. *Nat Med* 2014; **20**: 1410–1416.
- Garcia B, Rodriguez R, Angulo I, Heath AW, Howard MC, Subiza JL. Differential effects of transforming growth factor-beta 1 on IgA vs. IgG2b production by lipopolysaccharide-stimulated lymph node B cells: a comparative study with spleen B cells. *Eur J Immunol* 1996; **26**: 2364–2370.
- Randall KL, Lambe T, Johnson AL, Treanor B, Kucharska E, Domaschenz H *et al*. Dock8 mutations cripple B cell immunological synapses, germinal centers and long-lived antibody production. *Nat Immunol* 2009; **10**: 1283–1291.
- Baumgarth N. The double life of a B-1 cell: self-reactivity selects for protective effector functions. *Nat Rev Immunol* 2011; **11**: 34–46.
- Pillai S, Cariappa A, Moran ST. Positive selection and lineage commitment during peripheral B-lymphocyte development. *Immunol Rev* 2004; **197**: 206–218.
- Alhakeem SS, Sindhava VJ, McKenna MK, Gachuki BW, Byrd JD, Muthusamy N *et al*. Role of B cell receptor signaling in IL-10 production by normal and malignant B-1 cells. *Ann NY Acad Sci USA* 2015; **1362**: 239–249.
- Sindhava V, Woodman ME, Stevenson B, Bondada S. Interleukin-10 Mediated autoregulation of murine B-1 B-cells and its role in *Borrelia hermsii* infection. *PLoS ONE* 2010; **5**: e11445.
- Duan B, Morel L. Role of B-1a cells in autoimmunity. *Autoimmun Rev* 2006; **5**: 403–408.
- Klocke K, Sakaguchi S, Holmdahl R, Wing K. Induction of autoimmune disease by deletion of CTLA-4 in mice in adulthood. *Eur J Immunol* 2016; **46**: 770–770.
- Wing JB, Ise W, Kurosaki T, Sakaguchi S. Regulatory T cells control antigen-specific expansion of Tfh cell number and humoral immune responses via the coreceptor CTLA-4. *Immunity* 2014; **41**: 1013–1025.
- Sage PT, Paterson AM, Lovitch SB, Sharpe AH. The coinhibitory receptor CTLA-4 controls B cell responses by modulating T follicular helper, T follicular regulatory, and T regulatory cells. *Immunity* 2014; **41**: 1026–1039.
- Hou T, Verma N, Wanders J, Kennedy A, Soskic B, Janman D *et al*. Identifying functional defects in patients with immune dysregulation due to LRBA and CTLA-4 mutations. *Blood* 2017; **129**: 1458–1468.
- Paterson AM, Lovitch SB, Sage PT, Juneja VR, Lee Y, Trombley JD *et al*. Deletion of CTLA-4 on regulatory T cells during adulthood leads to resistance to autoimmunity. *J Exp Med* 2015; **212**: 1603–1621.

- 42 Tze LE, Horikawa K, Domaschensch H, Howard DR, Roots CM, Rigby RJ *et al*. CD83 increases MHC II and CD86 on dendritic cells by opposing IL-10-driven MARCH1-mediated ubiquitination and degradation. *J Exp Med* 2011; **208**: 149–165.
- 43 Lam LT, Wright G, Davis RE, Lenz G, Farinha P, Dang L *et al*. Cooperative signaling through the signal transducer and activator of transcription 3 and nuclear factor-kappa B pathways in subtypes of diffuse large B-cell lymphoma. *Blood* 2008; **111**: 3701–3713.
- 44 Bannard O, McGowan SJ, Ersching J, Ishido S, Victora GD, Shin JS *et al*. Ubiquitin-mediated fluctuations in MHC class II facilitate efficient germinal center B cell responses. *J Exp Med* 2016; **213**: 993–1009.
- 45 Phan TG, Amesbury M, Gardam S, Crosbie J, Hasbold J, Hodgkin PD *et al*. B cell receptor-independent stimuli trigger immunoglobulin (Ig) class switch recombination and production of IgG autoantibodies by anergic self-reactive B cells. *J Exp Med* 2003; **197**: 845–860.
- 46 Mombaerts P, Iacomini J, Johnson RS, Herrup K, Tonegawa S, Papaioannou VE. Rag-1-deficient mice have no mature lymphocytes-B and lymphocytes-T. *Cell* 1992; **68**: 869–877.
- 47 Zajac AJ, Blattman JN, Murali-Krishna K, Sourdive DJD, Suresh M, Altman JD *et al*. Viral immune evasion due to persistence of activated T cells without effector function. *J Exp Med* 1998; **188**: 2205–2213.
- 48 Parish IA, Marshall HD, Staron MM, Lang PA, Brustle A, Chen JH *et al*. Chronic viral infection promotes sustained Th1-derived immunoregulatory IL-10 via BLIMP-1. *J Clin Invest* 2014; **124**: 3455–3468.
- 49 Johnston RJ, Poholek AC, DiToro D, Yusuf I, Eto D, Barnett B *et al*. Bcl6 and Blimp-1 are reciprocal and antagonistic regulators of T follicular helper cell differentiation. *Science* 2009; **325**: 1006–1010.



This work is licensed under a Creative Commons Attribution-NonCommercial-ShareAlike 4.0 International License. The images or other third party material in this article are included in the article's Creative Commons license, unless indicated otherwise in the credit line; if the material is not included under the Creative Commons license, users will need to obtain permission from the license holder to reproduce the material. To view a copy of this license, visit <http://creativecommons.org/licenses/by-nc-sa/4.0/>

© The Author(s) 2017

The Supplementary Information that accompanies this paper is available on the Immunology and Cell Biology website (<http://www.nature.com/icb>)